The relevance of conservation for stability and accuracy of numerical methods for fluid-structure interaction

C. Michler *, E.H. van Brummelen, S.J. Hulshoff, R. de Borst

Delft University of Technology, Faculty of Aerospace Engineering,
P.O. Box 5058, NL-2600 GB Delft, The Netherlands

Abstract

Numerical simulation of fluid-structure interactions has typically been done using partitioned solution methods. However, partitioned methods are inherently non-conservative and generally numerically unstable. The deficiencies of partitioned methods have motivated the investigation of monolithic solution methods. Conservation is possible for monolithic methods, the conditions have recently been presented in Ref. [1]. In the present paper we investigate the relevance of maintaining conservation for a model fluid-structure interaction problem, viz., the piston problem. To distinguish the effect of the error induced by the interface coupling from the fluid and structure discretization errors, we use fluid subcycling and an exact time-integration method for the structure. A comparison between conservative and non-conservative monolithic methods as well as partitioned methods is made. We show that maintaining conservation has considerable impact on the stability and accuracy of the numerical method. These results also indicate that only for a conservative monolithic scheme the improvement in accuracy over partitioned methods warrants the computational cost associated with a monolithic solution. Moreover, we illustrate the implications that particular combinations of fluid and structure discretizations can have on the conservation properties of the fluid-structure interaction problem.

Key words: fluid-structure interaction, monolithic schemes, partitioned schemes, space-time formulation, time-discontinuous Galerkin method, energy conservation, numerical stability, accuracy

* Corresponding author.
Email address: C.Michler@LR.TUDelft.nl (C. Michler).

1 Introduction

There is an increasing demand for the accurate numerical solution of fluid-structure interaction problems arising in many engineering disciplines, such as aerospace engineering [2,3], civil engineering [4,5] and bio-mechanics [6]. Numerical solution methods for fluid-structure interaction typically employ partitioning. In a partitioned method, the fluid and the structure equations are alternatingly integrated in time and the kinematic and dynamic interface conditions are enforced asynchronously; see, e.g., Refs. [7,8,9]. The benefits and deficiencies of partitioned methods are discussed in Ref. [7]. The essential disadvantage of partitioning is the inherent loss of the conservation properties of the continuum fluid-structure system. Partitioned methods only satisfy conservation in an asymptotic sense, i.e., for vanishing mesh width. Although the order of the error incurred by a partitioned solution can be improved by predictors (see Refs. [9,10,11]), partitioned methods are never exactly conservative. In general, they are energy increasing and, hence, numerically unstable; see, e.g., Refs. [8,10].

The deficiencies of partitioned methods have motivated the investigation of monolithic methods, which treat the interaction of the fluid and the structure at the interface synchronously. The discretized equations are then typically solved by multiple fluid-structure iterations, also referred to as subiterations; see, e.g., Refs. [12,13,14]. This approach enables software modularity also for monolithic solution methods, i.e., the use of separate fluid and structure solvers. The computational cost per time step of a monolithic scheme is higher than the one associated with a partitioned scheme. On the other hand, only monolithic schemes can maintain the conservation properties. However, conservation is not immediate. Conservation is only trivially satisfied under restrictive compatibility conditions, see Ref. [1]. Recently, a new discretization based on coincidence conditions has been derived in Ref. [1], which ensures conservation also under incompatibility.

In the present work, we investigate the effect of maintaining conservation on the stability and accuracy of numerical methods for fluid-structure interaction. For this purpose, we compare conservative and non-conservative monolithic methods by numerical experiments with a prototypical fluid-structure interaction problem, viz., the piston problem from Ref. [15]. This model problem allows for an analytical solution of the structural equation, which enables us to perform the structural time integration exactly. Fluid discretization errors can be reduced using fluid subcycling. This combination allows us to study the effect of maintaining conservation at the interface separately.

Next, we investigate the effect of the numerical evaluation error in the solution of the coupled fluid-structure system. Partitioned as well as monolithic solution methods can employ subiteration. Partitioned schemes perform only a single subiteration, i.e., one fluid and structure solution per time step. Partitioned schemes

therefore do not solve the coupled fluid-structure system exactly and, hence, incur a numerical evaluation error. Monolithic schemes repeat subiterations until a certain tolerance criterion is satisfied, which ensures that the numerical evaluation error is smaller than fluid and structure discretization errors. In our numerical experiments, we show that in case of a partitioned solution method the numerical evaluation error can compromise stability and accuracy.

Finally, we investigate the implications that particular combinations of fluid and structure discretizations can have on the conservation properties. We consider different discretization methods for the structure, viz., the trapezoidal method and a time-discontinuous Galerkin method, coupled to a time-discontinuous Galerkin discretization of the fluid equations.

The contents of this paper are organized as follows : Section 2 describes the governing equations of the piston problem. Section 3 presents the discretization methods employed for fluid and structure as well as the conditions for maintaining conservation at the interface. In Section 4 we analyse the trapezoidal and the time-discontinuous Galerkin method for the structural time integration. In Section 5 we present numerical experiments and results. Section 6 contains concluding remarks.

2 Governing equations

This section presents the formulation of the piston problem from Ref. [15]. The governing equations of the continuum system for the fluid and the structure are introduced. Section 2.3 establishes the kinematic and dynamic conditions at the fluid-structure interface.

2.1 Fluid

The fluid is described by the one-dimensional Euler equations for compressible flow :

$$\frac{\partial U}{\partial t} + \frac{\partial F}{\partial x} = 0, \tag{1}$$

where $U = (\rho, \rho u, \rho e)$ is the state vector of conservative variables, and $F = (\rho u, \rho u^2 + p_f, \rho u e + p_f u)$ is the flux vector. ρ denotes the density, u is the velocity, p_f is the fluid pressure and e is the total energy density, respectively. The equation system is closed by the state equation for a perfect gas :

$$p_f = (\gamma - 1)\left(\rho e - \frac{1}{2}\rho u^2\right), \tag{2}$$

where γ denotes the ratio of specific heats (assumed to be 1.4 for the numerical experiments).

2.2 *Structure*

The structure is represented by a one-degree-of-freedom model (Fig. 1), which is described by the following differential equation :

$$m\ddot{z} + kz = p_s - p_0 =: \theta, \tag{3}$$

with the initial conditions :

$$z(t=0) = z_0, \tag{4a}$$

$$\dot{z}(t=0) = v_0, \tag{4b}$$

where z denotes the structural displacement, m the mass and k the spring-stiffness of the piston model, p_s is the pressure received by the structure from the fluid and p_0 is the atmospheric pressure. For the forcing term, $p_s - p_0$, we have introduced the notation θ. A superimposed dot denotes differentiation with respect to time. The surface of the piston is assumed to have a unit area.

2.3 *Interface conditions*

The interface conditions for the fluid-structure system can be expressed as a dynamic condition and two kinematic conditions. Dynamic equilibrium at the interface requires the pressure to be equal at either side of the interface:

$$p_s = p_f. \tag{5}$$

The first kinematic condition requires that the position of the fluid boundary is equal to its reference position, l_0, plus the structural displacement. The second kinematic condition requires that the fluid velocity at the boundary is equal to the velocity of the moving boundary. This can be expressed as follows :

$$l = l_0 + z, \tag{6a}$$

$$u = \dot{l}. \tag{6b}$$

The conditions for conservation of mass, momentum and energy at the fluid-structure interface can be expressed as the requirement that the corresponding fluxes on either side of the interface are equal. In particular,

$$\rho(u - \dot{l}) = 0, \tag{7}$$

$$\rho u(u - \dot{l}) + p_f = p_s, \tag{8}$$

$$\rho e(u - \dot{l}) + p_f u = p_s v, \tag{9}$$

with v denoting the structural velocity. Notice that the above conditions hold if the interface conditions, Eqs. (5)–(6), are satisfied.

3 Discretization

This section presents the discrete approximations to the continuum equations given in the previous section. Section 3.1 briefly describes the fluid discretization. For details of the method we refer to Refs. [16,17]. The considered structural representation consists of a one-degree-of-freedom model, and therefore only time discretization is required. Section 3.2 deals with the different structural time integration methods considered: Section 3.2.1 introduces the analytical solution to the structure equation. In the absence of discretization errors in the structure, this method is used to investigate the effect of maintaining conservation at the fluid-structure interface and to compare monolithic and partitioned schemes. In practice, however, an analytical solution for the structure is not available. To illustrate the implications that the choice of the structural discretization can have on the conservation properties of the fluid-structure interaction problem, we also consider the trapezoidal method and the time-discontinuous Galerkin method, presented in Sections 3.2.2 and 3.2.3, respectively. Section 3.3 outlines the conditions for maintaining conservation at the fluid-structure interface.

3.1 Fluid discretization

Problems of fluid-structure interaction involve moving boundaries and interfaces, which results in a deformation of the fluid domain in time. It then becomes necessary to perform the integration of the fluid equations on a moving mesh, which requires the incorporation of a Lagrangian description into the typically Eulerian fluid formulation. Conventional discretization techniques which are based on a separate space and time discretization of the fluid equations commonly use the Arbitrary Lagrangian-Eulerian (ALE) technique; see, e.g., Ref. [18]. Another, more elegant way of treating deforming domains is the space-time formulation of the fluid equations, as was already recognized in Ref. [19] and illustrated with various examples in, e.g., Refs. [19,20].

In the space-time formulation the variational statement is written over the space-time domain and, hence, a deformation of the spatial domain in time is accounted for automatically. The space-time formulation is in fact analogous to the ALE formulation; see Ref. [21]. As the ALE formulation is based on a separate space and time discretization, maintaining the accuracy on a moving mesh requires compliance with an additional constraint, the so-called Geometric Conservation Law, whereas the space-time formulation satisfies the Geometric Conservation Law inherently; see, e.g., Ref. [22].

We employ in our work the space-time formulation, which treats spatial and temporal derivatives uniformly, i.e., by the same discretization method. We use a standard

time-discontinuous Galerkin method with piecewise-linear trial and test functions, which are continuous in space but discontinuous in time at the space-time slab interfaces. This separates the computational task into the sequential solution of multiple space-time slabs and is attractive for adaptation, in that it offers the possibility of changing the spatial discretization from one space-time slab to the next. Information is propagated across space-time slab interfaces by weakly enforced initial conditions.

The conservation form of the fluid equations is discretized in primitive variables, (p_f, u, T) with T denoting the absolute temperature, which simplifies the implementation of boundary conditions and, in particular, the coupling to the structure. For the discretization in primitive variables we refer to Ref. [17]. The formulation can be augmented with a least-squares term to improve the stability of the Galerkin formulation.

For the variational formulation and the definition of the least-squares operator we refer to Refs. [16,17,19]. A Fourier stability and accuracy analysis of the space-time Galerkin least-squares method is presented in Ref. [23]. The resulting system of non-linear equations is solved by a predictor multi-corrector method, similar to the one described in Ref. [16].

3.2 Structural time integration

3.2.1 Exact structural time integration

The motion of the piston is described by the initial value problem, Eqs. (3)–(4). For the approximation of the fluid pressure we use shape functions which are piecewise linear in time. We approximate the forcing term of the structure also by a piecewise-linear function. The variation of the forcing term within the generic time interval $[0, \Delta t]$ is then of the form

$$\theta = \theta_0 + \frac{\theta_1 - \theta_0}{\Delta t}\, t, \tag{10}$$

where the subscripts $_0$ and $_1$ refer to the values at the beginning and end of the time interval, respectively. Because θ is a linear function in our discretization, the second-order ordinary differential equation can be solved analytically. The solution of the initial value problem, Eqs. (3)–(4), subject to Eq. (10), is then

$$z(t) = \left(z_0 - \frac{\theta_0}{k}\right) \cos\left(\sqrt{\frac{k}{m}}t\right) + \frac{\left(v_0 - \frac{\theta_1 - \theta_0}{\Delta t k}\right)}{\sqrt{\frac{k}{m}}} \sin\left(\sqrt{\frac{k}{m}}t\right) + \frac{\theta_0 + \frac{\theta_1 - \theta_0}{\Delta t}\, t}{k}. \tag{11}$$

Given the values of the forcing term at either time level, θ_0 and θ_1, the structural displacement can be calculated from Eq. (11).

3.2.2 Trapezoidal method

The trapezoidal method is a common discretization method for ordinary-differential equations. It is attractive because of its simplicity and its conservation of energy in the absence of exterior forces; see Ref. [24]. Trapezoidal time integration corresponds to a Newmark method (see Ref. [24]) with the parameter choice $\beta = \frac{1}{4}$ and $\gamma = \frac{1}{2}$. This method is also referred to as the *average acceleration method.*

3.2.3 Time-discontinuous Galerkin method

Below, we consider a velocity-based, time-discontinuous Galerkin discretization for the structural time integration. Using the same discretization method for the structure as for the fluid allows us to treat structure and fluid in a unified framework and simplifies fluid-structure coupling. The time-discontinuous Galerkin method employs trial and test functions which are discontinuous in time at the time-slab interfaces. In particular, we use a piecewise-linear approximation of the velocity. In the following, $+$ and $-$ signs are used to indicate from which side the discontinuity is approached. To formulate the structural equation in terms of velocity, v, as a primary unknown, we rewrite Eq. (3) as

$$m\dot{v} + k\left(z_{t=0} + \int_{t=0}^{t} v(\xi)d\xi\right) = \theta. \tag{12}$$

The variational statement for a single time-slab $[t_n^+, t_{n+1}^-]$ is then defined as follows: Find a linear function v^h such that

$$\begin{aligned} &\omega^h(t_{n+1}^-)mv^h(t_{n+1}^-) - \omega^h(t_n^+)mv^h(t_n^+) - \int_{t_n^+}^{t_{n+1}^-} \dot{\omega}^h mv^h \, dt \\ &+k\int_{t_n^+}^{t_{n+1}^-} \omega^h z^h(t_n^+) \, dt + k\int_{t_n^+}^{t_{n+1}^-} \omega^h \left(\int_{t_n^+}^{t} v^h(\xi)d\xi\right) \, dt = \int_{t_n^+}^{t_{n+1}^-} \omega^h \theta^h \, dt \end{aligned} \tag{13}$$

for all linear test functions ω^h. Eq. (13) has been obtained through integration-by-parts. The initial condition for displacement,

$$z^h(t_n^+) = z^h(t_n^-), \tag{14}$$

is enforced strongly, and therefore displacement is continuous at the time-slab interfaces. The initial condition for velocity is only weakly enforced by the jump condition,

$$\omega^h(t_n^+)(v^h(t_n^+) - v^h(t_n^-)) = 0, \tag{15}$$

allowing for discontinuous velocity at the time-slab interfaces. Introducing Eqs. (14)–(15) in Eq. (13), the variational statement for a single time-slab, including the initial

conditions, is reformulated as : Find a linear function v^h such that

$$\begin{aligned}\omega^h(t_{n+1}^-)mv^h(t_{n+1}^-) - \int_{t_n^+}^{t_{n+1}^-} \dot{\omega}^h mv^h \, dt + k\int_{t_n^+}^{t_{n+1}^-} \omega^h \left(\int_{t_n^+}^{t} v^h(\xi)d\xi\right) dt \\ = \omega^h(t_n^+)mv^h(t_n^-) - k\int_{t_n^+}^{t_{n+1}^-} \omega^h z^h(t_n^-)\, dt + \int_{t_n^+}^{t_{n+1}^-} \omega^h \theta^h \, dt\end{aligned} \tag{16}$$

for all linear test functions ω^h.

3.3 Discrete interface conditions

In this section we describe the conditions which ensure conservation at the interface for a monolithic scheme, see also Ref. [1]. In Section 5.2 we exemplify conservative and non-conservative schemes and investigate the relevance of maintaining conservation at the interface.

Eqs. (5)–(6) constitute the conditions for the continuum system, which imply conservation of mass, momentum and energy at the fluid-structure interface. Their discrete counterparts can be written correspondingly. It then follows that conservation is only trivially maintained under restrictive compatibility conditions on the approximation spaces of fluid and structure variables, such as identical approximation spaces of the pressure at either side of the interface and a discrete fluid and structure boundary which matches exactly. These requirements are prohibitively restrictive for practical use.

Recently, it was pointed out in Ref. [1] that conservation can be ensured even under incompatibility; the requirements are based on coincidence conditions and will be presented in the following. From Eq. (7) it follows that a basic condition for conservation at the interface is :

$$u^h = \dot{l}^h, \tag{17}$$

i.e., the fluid velocity at the boundary equals the fluid-boundary velocity. The requirements for energy conservation under incompatibility are derived from the integral form of Eq. (9), expressing conservation in an integral sense, i.e., per time interval. Subject to Eq. (17) and using integration-by-parts, they are expressed for a generic time interval $[0, \Delta t]$ as follows :

$$\int_0^{\Delta t} \phi^h(p_f^h - p_s^h)dt = 0 \quad \forall \phi^h \in \mathrm{span}\{1, t\}, \tag{18a}$$

$$l^h(0) = l_0 + z^h(0), \tag{18b}$$

$$l^h(\Delta t) = l_0 + z^h(\Delta t), \tag{18c}$$

$$\int_0^{\Delta t} \lambda^h \left(\dot{l}^h - (\dot{l}_0 + \dot{z}^h)\right) dt = 0 \quad \forall \lambda^h \in \mathrm{span}\{1\}. \tag{18d}$$

Notice that the fluid boundary and the structure are required to coincide only at

the beginning and end of a time interval, as expressed by the coincidence conditions, Eqs. (18b) and (18c). The fluid-boundary displacement is continuous from one space-time slab to the next, which enables matching meshes at space-time slab interfaces and, hence, avoids interpolation of the jump-term. If Eqs. (17)–(18) are simultaneously satisfied, mass, momentum and energy are conserved at the fluid-structure interface.

The discussion of conservative coupling at the fluid-structure interface also involves the issue of the variables used for the fluid discretization. Variables with a non-polynomial representation of the fluid pressure and velocity, such as entropy variables [16] for example, directly lead to an incompatibility with the approximation spaces used in the structure. Conservation at the interface still can be maintained provided that Eqs. (17)–(18) hold. However, the evaluation of the integrals involves non-linear transformations and therefore is more complicated in that case. We use primitive variables, (p_f, u, T), for the fluid discretization instead, which simplifies the fluid-structure coupling.

In the context of our investigation of conservative fluid-structure coupling, consideration of the conservation properties of the fluid and structure discretization separately is also relevant. The Galerkin discretization of the fluid equations in conservation form is globally conservative for any choice of variables, see Refs. [17,25]. The conservation properties of the structure discretization will be investigated in the following section.

4 Analysis of the structural time-integration methods

To illustrate the implications that the choice of the structural discretization can have on the conservation properties of the fluid-structure interaction problem, we consider the trapezoidal method and the time-discontinuous Galerkin method, presented in Sections 3.2.2 and 3.2.3, respectively. In this section, we examine the phase and amplitude characteristics of the discretization error of the respective methods. Moreover, we assess whether the coupling of the structural time-integration methods to the fluid discretization conserves momentum and energy at the interface.

4.1 Analysis of the trapezoidal method

4.1.1 Amplitude and phase error

The amplitude and phase characteristics of the time-integration methods are determined for the unforced structure by means of the techniques described in, e.g.,

Refs. [24,26]. The errors are plotted in Figs. 2 and 3 versus the size of the time step. Here, an oscillation period is equal to a unit time. Fig. 2 shows that trapezoidal time integration is void of amplitude error, and consequently, preserves the amplitude of the structural oscillation exactly. Fig. 3, however, shows that the trapezoidal time integration method has a considerable phase error.

4.1.2 Energy conservation

The trapezoidal method can be shown to be energy conservative for an unforced structure, see Ref. [24]. To assess energy conservation in the presence of a forcing term, we start from the continuum equation, Eq. (3). Multiplying Eq. (3) by $\dot{z}$ and invoking integration-by-parts on the left-hand side gives the following energy statement:

$$\left[\frac{1}{2}m\dot{z}^2 + \frac{1}{2}kz^2\right]_{t_n}^{t_{n+1}} = \int_{t_n}^{t_{n+1}} \dot{z}\theta dt. \tag{19}$$

Defining E as the sum of kinetic and strain energy, according to $E := \frac{1}{2}m\dot{z}^2 + \frac{1}{2}kz^2$, we can rewrite Eq. (19) as

$$E_{n+1} - E_n = \int_{t_n}^{t_{n+1}} \dot{z}\theta dt. \tag{20}$$

To determine the conservation properties of the trapezoidal method, we note that the energy E at time level $n+1$ can be written in the following form :

$$E_{n+1} = \begin{pmatrix} v_{n+1} \\ d_{n+1} \end{pmatrix}^T \cdot \begin{bmatrix} \frac{m}{2} & 0 \\ 0 & \frac{k}{2} \end{bmatrix} \cdot \begin{pmatrix} v_{n+1} \\ d_{n+1} \end{pmatrix}. \tag{21}$$

Manipulation of the expressions for the trapezoidal method yields a relation for (v_{n+1}, d_{n+1}) in terms of (v_n, d_n). Eq. (21) can then be rewritten as

$$E_{n+1} - E_n = \Delta t \left(\frac{v_{n+1} + v_n}{2}\right)\left(\frac{\theta_{n+1} + \theta_n}{2}\right). \tag{22}$$

From a comparison of Eqs. (20) and (22) it follows that

$$\int_{t_n}^{t_{n+1}} \dot{z}\theta dt = \Delta t \left(\frac{v_{n+1} + v_n}{2}\right)\left(\frac{\theta_{n+1} + \theta_n}{2}\right), \tag{23}$$

i.e., in the trapezoidal method the integral is approximated by the midpoint rule. Only in the specific case that θ is constant and v is linear, or vice versa, is the integral evaluated exactly by the midpoint rule. We infer that trapezoidal time integration does not generally conserve energy in the presence of a forcing term.

More specifically, we are interested in the conservation properties of the trapezoidal time integration method when coupled to the fluid discretization. Strong coupling

for the pressures p_f, p_s and the velocities u, v at either side of the interface implies that these quantities have the same value at each time level. The coupling to the time-discontinuous fluid discretization implies that the average acceleration is computed from a discontinuous forcing term, θ. Structural displacement and velocity, however, are continuous from one time-slab to the next and, consequently, kinetic and strain energy of the structure are conserved from one time-slab to the next. Provided that Eq. (17) holds, mass conservation of the fluid at the interface is immediate and the equilibrium of forces at the interface implies conservation of momentum.

To assess energy conservation at the interface, the change in energy within a time-slab is compared at either side of the interface: For the structure integrated by trapezoidal time integration we refer to Eq. (22). For the fluid we obtain :

$$\begin{aligned} E_{n+1} - E_n &= \int_{t_n^+}^{t_{n+1}^-} p_f \; u \; dt \\ &= \frac{1}{6}\Delta t \left(2p_{f,n+1}u_{n+1} + p_{f,n+1}u_n + p_{f,n}u_{n+1} + 2p_{f,n}u_n\right), \end{aligned} \tag{24}$$

where for velocity u and pressure p_f linear-in-time shape functions have been assumed. The calculated change of energy across a time-slab on the structure side (Eq. (22)) is different from the fluid side (Eq. (24)). Therefore we infer that trapezoidal time integration does not conserve energy at the interface.

4.2 Analysis of the time-discontinuous Galerkin method

4.2.1 Amplitude and phase error

The amplitude and phase error of the discontinuous Galerkin time integration method are determined in a similar manner as in Section 4.1.1. The errors are plotted in Figs. 4 and 5. Fig. 4 shows that the time-discontinuous Galerkin method has an amplitude error and, hence, does not preserve exactly the amplitude. Its phase error, however, is much smaller than for the trapezoidal method, as can be seen by comparing Fig. 5 to Fig. 3.

4.2.2 Energy conservation

As velocity is contained in the test-space, energy conservation within each time-slab is implied by Eq. (16). However, due to the weak enforcement of the initial condition for velocity, Eq. (15), this discretization loses energy between two time-slabs.

If the time-discontinuous Galerkin method is used for both the fluid and the structure, the polynomial representation of velocity and pressure can be made identical

on either side of the interface. In this case the compatibility conditions are satisfied, and therefore both momentum and energy are conserved at the fluid-structure interface. Alternatively, the coincidence and orthogonality conditions, Eq. (18), can be imposed to maintain conservation under incompatibility, e.g., due to subcycling.

5 Numerical experiments

In this section we present numerical experiments and results for a prototypical fluid-structure interaction problem, viz., the piston problem. However, it is anticipated that the main conclusions extend *in abstracto* to more complicated fluid-structure interaction problems.

5.1 Settings of the numerical experiments

5.1.1 Parameters of the piston problem

The parameters of the piston problem are given in Table 1, where ω_{fs} denotes the frequency of the fluid-structure system. They are similar to the settings used in Ref. [15].

We denote the characteristic time-scales of fluid, structure and fluid-structure system by

$$T_f = \frac{2l_0}{c}, \qquad T_s = 2\pi\sqrt{\frac{m}{k}}, \qquad T_{fs} = \frac{2\pi}{\omega_{fs}}, \tag{25}$$

respectively, where c is the speed of sound. Introducing the following non-dimensional time-scale ratios:

$$\frac{T_f}{T_{fs}} = 0.34, \qquad \frac{T_s}{T_{fs}} = 3.44 \tag{26}$$

and the non-dimensional mass ratio of fluid and structure :

$$\mu = \frac{\rho l_0}{m} = 1.63 \tag{27}$$

we can describe the problem in terms of non-dimensional quantities. For the current parameters, the characteristic time-scale for the structure is much greater than the fluid time-scale, which implies that the fluid behaviour can be considered as quasi-steady. Moreover, the mass ratio of fluid and structure is of order one, which implies that fluid and structure contribute equally to the dynamics of the system.

The computation is started from initial conditions which are derived from the solution of the linearized problem with an initial structural displacement of $z_0 = 0.01$. The non-dimensional quantities are chosen such that one oscillation period is equal to a unit time.

5.1.2 Parameters of the discretization

The initial structural displacement is sufficiently small for the fluid to behave quasi-linearly, in which case the least-squares stabilization is not necessary. It is deactivated to reduce the dissipation in the fluid.

The fluid discretization is done by the time-discontinuous Galerkin method, which employs linear-in-time shape functions and is therefore formally second-order time accurate. When investigating the effect of the discretization error due to the coupling we have to ensure that the fluid discretization error is sufficiently small. We achieve this by fluid subcycling, i.e., the fluid discretization uses time steps Δt_f, which are smaller than the time steps of the structural discretization, Δt_s. The ratio $\eta = \frac{\Delta t_s}{\Delta t_f}$, $\eta \in \mathbb{N}$ is called the subcycling factor. In the numerical experiments we use a subcycling factor of $\eta = 8$, unless stated otherwise.

5.2 Conservative vs. non-conservative monolithic methods

This section investigates the effect of maintaining conservation at the fluid-structure interface for monolithic methods by comparing numerical results for conservative and non-conservative methods. The monolithic solution methods repeat subiterations until the numerical evaluation error is smaller than fluid and structure discretization errors. Moreover, in order to ensure that the error incurred by non-conservative interface coupling is dominant, we use the exact structural solution from Section 3.2.1 and subcycling in the fluid.

5.2.1 Coupling methods

We consider three coupling methods, which all naturally conserve mass at the interface, but differ in their conservation properties for energy and momentum. Nevertheless, all three discretizations are consistent and second-order time accurate, as will be shown in Section 5.2.2. Therefore, the preference of one method over the other can only be motivated by the intention of maintaining conservation.

- method A :
  This method satisfies Eq. (18). Therefore, the fluid-structure coupling is fully conservative.
- method B :
  This method satisfies Eqs. (18b)–(18d), but not Eq. (18a). p_s within a time interval $t \in [0, T]$ is calculated in an ad-hoc but consistent way by using a linear interpolation that coincides with p_f at the beginning and end of the time interval, i.e.,

$$p_s(t) = p_f(t=0) + \frac{t}{T}\Big(p_f(t=T) - p_f(t=0)\Big). \tag{28}$$

This finite-difference discretization is typically used in combination with subiteration methods; see, e.g., Ref. [13]. However, this discretization does neither conserve energy nor momentum at the fluid-structure interface.

- method C :
  This method satisfies Eq. (18a), but not Eqs. (18b)–(18d). For the discrete fluid boundary displacement, z_f^h, a quadratic function is assumed, which is determined from the requirement that z_f^h is continuous from one fluid time-slab to the next, in combination with the following orthogonality condition:

$$\int_0^{\Delta t} \lambda^h \left((z_f^h - z_{f,0}^h) - (z_s^h - z_{s,0}^h) \right) dt = 0 \quad \forall \lambda^h \in \mathrm{span}\{1, t\}. \tag{29}$$

  z_s^h denotes the approximation to the displacement of the structure, and the subscript $_0$ refers to the values at the beginning of a time interval. Fluid boundary and structure only coincide initially at time $t = 0$, but can deviate henceforth. This coupling method does not conserve energy at the interface, but it conserves momentum, as it satisfies Eq. (18a).

As we employ fluid subcycling, interpolation of the kinematic boundary conditions for the fluid, i.e., the structural displacement and velocity, is necessary at all time levels of the fluid which do not coincide with the time levels of the structure, i.e., at $\Delta t_f \ldots (\eta - 1)\Delta t_f$. The interpolation of the structural solution is done according to Eq. (18) for methods A and B; for method C Eq. (29) is employed.

5.2.2 Numerical results

Fig. 6 compares the numerical solution for the structural displacement obtained with the coupling methods A, B and C. An oscillation period is resolved by 10 structural time steps or, equivalently, by 80 time steps in the fluid. The figure clearly shows that the amplitude of the non-conservative method B decays rapidly, whereas the amplitude of the conservative method A remains apparently unchanged. The modulation of the solution computed with method B can be attributed to interfering waves : The initial conditions correspond to a periodic solution of the continuum problem, but do not generally yield a periodic discrete solution. Moreover, we notice a considerable phase error in the solution computed with method B. The amplitude computed with method C grows in time, and the solution appears to be numerically unstable, even though method C is a monolithic scheme. The latter is noteworthy, because the fact that monolithic schemes can be numerically unstable does not seem to be widely known.

The results of a mesh refinement study are shown in Fig. 7. The L_2-norm of the error in the computed structural displacement is plotted versus the size of the structural time step for $\Delta t_s = 2^{-3} \ldots 2^{-7}$. The reference solution was obtained with the conservative monolithic method A for a structural time step $\Delta t_s = 2^{-8}$.

Fig. 7 confirms that the methods are second-order time accurate. Moreover, it is apparent that the conservative method A is by more than two orders of magnitude more accurate than the non-conservative methods B and C. Hence, for a given level of accuracy, the conservative method can afford much larger time steps than the non-conservative methods. We infer that maintaining conservation at the interface is an important requirement for the accuracy of the numerical solution. An additional computational cost is not incurred.

5.3 Monolithic vs. partitioned methods

In the previous section the importance of maintaining the conservation properties has been demonstrated. This issue also involves a discussion of partitioned and monolithic schemes, as the former are inherently non-conservative. In Section 5.3.1 we compare monolithic and partitioned schemes; similar investigations have been presented in Refs. [27,28,29]. In Refs. [27,28] the average acceleration method is used for the structural time integration, and Ref. [29] uses an Arbitrary Lagrangian Eulerian approach. Here, we compare numerical results for monolithic and partitioned schemes, using the exact structural time integration and a coupling strategy based on Eq. (18). This ensures conservation at the interface for a monolithic solution. The monolithic method is identical to method A of Section 5.2.

Our approach has the advantage that it isolates the effect of fluid and structure discretization errors from the numerical evaluation error. This allows us to study the effect of the latter separately, and to show the relevance of structural prediction for a partitioned scheme (Section 5.3.1). In Section 5.3.2 we investigate the temporal accuracy of monolithic and partitioned solution methods. Whereas the difference between the methods is also apparent without fluid subcycling for coarse time steps, we need to employ fluid subcycling when investigating the accuracy of the methods in order to reduce the effect of fluid dissipation. In general, fluid dissipation damps the solution and, hence, counteracts the amplification caused by the partitioned methods.

5.3.1 Comparing the effect of monolithic and partitioned methods

For the numerical experiments presented in this section the same time-step size is used for the fluid and structure discretizations. The size of the time step is indicated below the figures. Figs. 8–10 plot the structural displacement versus time for five cycles of oscillation. In Fig. 8 the amplitude computed with the partitioned scheme grows in time, whereas the amplitude computed with the monolithic scheme remains constant. This calculation uses 100 time steps per cycle. Next, we use a structural prediction according to Eq. (11) with values of the forcing term at the previous time level. When using a structural predictor for the partitioned scheme,

the growth in amplitude is substantially reduced so that partitioned and monolithic results visually coincide (Fig. 9, with the same number of time steps per cycle as in Fig. 8). Obviously, structural prediction can reduce the numerical evaluation error incurred in a partitioned solution. However, if the number of time steps per cycle is reduced, e.g., by a factor of ten (Fig. 10), the error in the amplitude computed with the partitioned scheme emerges again, in spite of the structural predictor. The amplification of the solution obtained with the partitioned method can be attributed to artificial energy production at the interface, which can induce numerical instability of the combined fluid-structure system; see, e.g., Refs. [8,10]. In practice, this imposes a restriction on the time-step size. The monolithic scheme does not become numerically unstable. Indeed, as it maintains exactly the conservation properties at the interface, it is unconditionally stable. In this case, there does not exist a restriction on the admissible time-step size for a monolithic scheme other than the required accuracy.

We note, however, that for a single-mode problem such as the one considered stability and accuracy are closely related. Only for multiple-mode problems stability and accuracy can be distinguished clearly. For partitioned schemes, the stability of modes with time scales smaller than one actually wants to resolve can impose a severe restriction on the admissible time-step size. On the other hand, for monolithic schemes there is no such stability restriction, but the time-step size is restricted by accuracy considerations only. This discussion is similar to the one about time-step restriction for explicit vs. implicit time-integration methods.

5.3.2 Grid refinement study

This subsection investigates the temporal accuracy of monolithic and partitioned schemes. We use the same settings as in Section 5.3.1. However, the subcycling ratio is set to 8.

The observed order of temporal accuracy is determined by

$$p = \ln\left(\frac{||z_{4\tau} - z_{2\tau}||}{||z_{2\tau} - z_{1\tau}||}\right) / \ln(2), \tag{30}$$

where p denotes the observed order of temporal accuracy and z the computed structural displacement on meshes of different structural time-step sizes (denoted by τ, 2τ and 4τ). The differences are measured in the L_2-norm.

As the fluid equations are formulated and discretized in space-time, refinement of the temporal mesh width requires a corresponding refinement of the spatial mesh width to obtain second-order convergence. If this is not done, the truncation error retains a mixed term, $\Delta t_f \Delta x$, which will produce only first-order convergence. For the current computations, the non-dimensional spatial mesh width in the fluid was taken equal to the temporal mesh width.

The computations were performed on a sequence of meshes of different time-step sizes. Table 2 shows the observed order of temporal accuracy for the monolithic method as well as for the partitioned method with and without structural prediction. The observed order of temporal accuracy shows the expected asymptotic behaviour, i.e., second-order accuracy for the monolithic method and for the partitioned method with prediction, and first-order accuracy for the partitioned method without prediction.

The monolithic method and the partitioned method with prediction have formally the same order of accuracy; the nature and magnitude of the dominant errors, however, is inherently different. Fig. 11 plots the error versus the time step for $\tau = 2^{-3} \dots 2^{-7}$, using the same reference solution as in Section 5.2.2. As the monolithic and the partitioned method differ only in the number of subiterations, we can infer from Fig. 11 that the numerical evaluation error in the partitioned solution is by several orders of magnitude larger than the fluid and structure discretization errors. Consequently, in a partitioned solution the numerical evaluation error can dominate other sources of error. From Fig. 11 it is clear that the partitioned method requires smaller time steps than the monolithic method for a specified error tolerance. Conversely, given a certain level of accuracy, a monolithic method can afford larger time steps than a partitioned method.

As the grid refinement study uses the same settings and reference solution as in Section 5.2, the accuracy of the partitioned method can be compared also to the accuracy of the non-conservative monolithic methods B and C; refer to Fig. 7. Although the non-conservative methods B and C are more accurate than the partitioned method with prediction, the gain in accuracy does not seem to justify the computational effort associated with a monolithic method. However, comparing the accuracy of a partitioned and a conservative monolithic discretization, it is clear from Fig. 11 that the latter is by more than three orders of magnitude more accurate. Hence, monolithic methods are much more accurate than partitioned methods, provided that they maintain conservation at the interface. In that case they warrant their higher computational cost and become computationally more efficient than partitioned methods, cf. Ref. [30].

5.4 Trapezoidal vs. discontinuous Galerkin time integration for the structure

This section demonstrates the implications of the adopted structural discretization methods. We consider the coupling of the time-discontinuous Galerkin discretization of the fluid equations with the time-discontinuous Galerkin and the trapezoidal time integration for the structure, respectively, and investigate the effect on accuracy for a monolithic solution.

The possibility of energy-conservative coupling has been investigated in Section 4.

The time-discontinuous Galerkin discretization for the structural time integration conserves momentum and energy at the fluid-structure interface. However, this method loses energy in between time-slabs due to the discontinuity in velocity. With the trapezoidal discretization for the structure, momentum is conserved at the interface, but not energy.

5.4.1 Grid refinement study

In the following, we assess the temporal accuracy for the structural time integration methods in a monolithic solution with fluid subcycling. Table 3 shows the observed order of temporal accuracy (determined as in Section 5.3.2) for trapezoidal and time-discontinuous Galerkin time integration.

Table 3 indicates that the trapezoidal time integration gives second-order time-accurate results in a monolithic solution. This was to be expected, as both the trapezoidal method and the fluid discretization are second-order time accurate, see Ref. [24]. The time-discontinuous Galerkin discretization for the structure uses linear-in-time shape functions for the velocity. The structural displacement is obtained by integration. Therefore this method is third-order time accurate in displacement. Indeed, we can observe third-order convergence for the Galerkin time integration, because the discretization errors in the fluid and at the interface are smaller than the discretization error in the structure due to fluid subcycling and conservative fluid-structure coupling, respectively. However, on even finer mesh sequences second-order time-accuracy is recovered, manifesting the second-order time-accuracy of the fluid discretization.

The different orders of the structural time integration methods also become apparent in Fig. 12, in which the error is plotted versus the size of the structural time step for $\tau = 2^{-3} \dots 2^{-7}$. We use the same reference solution as in Sections 5.2.2 and 5.3.2. The errors corresponding to the Galerkin method and to the trapezoidal method are markedly different. This difference emanates partly from the different structure discretization and partly from the different interface treatment. As the interface coupling is formally only second-order accurate, the observed third-order convergence behaviour of the Galerkin method indicates that conservative interface coupling introduces an error that is typically much smaller than the structural discretization error. Moreover, a comparison of Figs. 7 and 12 shows that the error in the fluid-structure coupling with the trapezoidal structural discretization is comparable to the error in the non-conservative monolithic methods. It appears that the error incurred by non-conservative coupling at the interface generally dominates the structural discretization error.

6 Conclusions

This paper investigates the relevance of maintaining conservation at the interface for the accuracy and stability of numerical methods for fluid-structure interaction. We considered conservative and non-conservative monolithic methods. To distinguish the effect of the error incurred by non-conservative interface coupling from the fluid and structure discretization errors, we used fluid subcycling and exact structural time integration. We also investigated the effect of the numerical evaluation error incurred by a partitioned solution method. Furthermore, we considered the implications of specific choices of the structural discretization method. Numerical results were presented for a one-dimensional model problem.

Comparing conservative and non-conservative monolithic methods, we showed that maintaining conservation at the interface results in a more accurate solution, at the same computational price. Moreover, we demonstrated that a violation of energy conservation can lead to numerical instability, even for monolithic methods.

The ability of monolithic methods to maintain conservation at the interface constitutes an essential advantage over partitioned methods. Conservative monolithic methods are unconditionally stable, whereas partitioned methods are typically unstable. Moreover, we showed that a conservative monolithic method is much more accurate than a partitioned method and, hence, can afford much larger time steps for the same level of accuracy. Our results also indicate that for non-conservative monolithic methods the improvement in accuracy over partitioned methods does not seem to warrant the additional computational cost.

To illustrate the implications of particular combinations of fluid and structure discretizations, we considered different discretization methods for the structure, viz., the trapezoidal method and a time-discontinuous Galerkin method. We showed that the trapezoidal time-integration method does not generally conserve energy for forced structures. Hence, it is non-conservative at the fluid-structure interface. In contrast, the time-discontinuous Galerkin discretization can maintain conservation at the interface. However, this method loses energy between time-slabs due to the discontinuity in velocity. Our results indicate that the error incurred by non-conservative interface coupling can dominate other sources of discretization error, whereas conservative interface coupling introduces an error that is generally much smaller than other error sources.

References

[1] E.H. van Brummelen, S.J. Hulshoff and R. de Borst, *Energy conservation under incompatibility for fluid-structure interaction problems*, Comput. Methods Appl.

Mech. Engrg.-(2003). (Accepted for publication). Preprint available at : http://www.em.lr.tudelft.nl/~brummelen/publications.html

[2] C. Farhat, P. Geuzaine, G. Brown, *Application of a three-field nonlinear fluid-structure formulation to the prediction of the aeroelastic parameters of an F-16 fighter*, Computers and Fluids, 32, (2003), 3–29.

[3] C. Farhat, P. Geuzaine, and C. Grandmont, *The Discrete Geometric Conservation Law and the Nonlinear Stability of ALE Schemes for the Solution of Flow Problems on Moving Grids*, Journal of Computational Physics, 174, (2001), 669–694.

[4] I. Robertson, S. J. Sherwin, and P. W. Bearman, *Prediction of flutter instability due to cross winds of the second forth road bridge*, in: Computational Fluid Dynamics '01: Proceedings of the ECCOMAS CFD Conference 2001, Swansea, Wales, U.K., 2001. on CD-rom.

[5] B. Hübner, E. Walhorn and D. Dinkler, *Numerical investigation to bridge aeroelasticity*, in: Proceedings of the Fifth World Congress on Computational Mechanics (WCCM V) (H. A. Mang, F. G. Rammerstorfer and J. Eberhardsteiner, eds.), Vienna University of Technology, Austria, July 7-12 2002. Available at : http://wccm.tuwien.ac.at

[6] M. Heil, *Stokes flow in an elastic tube - a large displacement fluid-structure interaction problem*, Int. J. Num. Methods Fluids, 28, (1998), 243–265.

[7] C.A. Felippa, K.C. Park, C. Farhat, *Partitioned analysis of coupled mechanical systems*, Comput. Methods Appl. Mech. Engrg., 190, (2001), 3247–3270.

[8] S. Piperno, C. Farhat, B. Larrouturou, *Partitioned procedures for the transient solution of coupled aeroelastic problems - Part I : Model problem, theory and two-dimensional applications*, Comput. Methods Appl. Mech. Engrg., 124, (1995), 79–112.

[9] S. Piperno, C. Farhat, *Partitioned procedures for the transient solution of coupled aeroelastic problems - Part II : energy transfer analysis and three-dimensional applications*, Comput. Methods Appl. Mech. Engrg., 190, (2001), 3147–3170.

[10] S. Piperno, *Explicit/implicit fluid/structure staggered procedures with a structural predictor and fluid subcycling for 2d inviscid aeroelastic simulations*, Int. J. Num. Methods Fluids, 25, (1997), 1207–1226.

[11] S. Piperno, C. Farhat, *Design and evaluation of staggered partitioned procedures for fluid-structure interaction simulations*, Tech. Rep. 3241, CERMICS-INRIA (1997).

[12] P. LeTallec, J.Mouro, *Fluid-structure interaction with large structural displacements*, Comput. Methods Appl. Mech. Engrg., 190, (2001), 3039–3067.

[13] J.J. Alonso, A. Jameson, *Fully-implicit time-marching aeroelastic solutions*, AIAA, 0056, (1994), 1–13.

[14] S.A. Morton, R.B. Melville, M.R. Visbal, *Accuracy and coupling issues of aeroelastic Navier-Stokes solutions on deforming meshes*, AIAA, 1085, (1997), 252–262.

[15] S. Piperno, *Simulation numérique de phénomènes d'interaction fluide-structure*, PhD thesis, Ecole Nationale des Ponts et Chaussées, France, (1995). (partly in French).

[16] F. Shakib, T.J.R. Hughes and Z. Johan, *A new finite element formulation for computational fluid dynamics: X. The compressible Euler and Navier-Stokes equations*, Comput. Methods Appl. Mech. Engrg., 89, (1991), 141–219.

[17] G. Hauke, T.J.R. Hughes, *A comparative study of different sets of variables for solving compressible and incompressible flows*, Comput. Methods Appl. Mech. Engrg., 153, (1998), 1–44.

[18] J. Donea, S. Guiliani and J.P. Halleux, *An arbitrary Lagrangian-Eulerian finite element method for transient dynamic fluid-structure interactions*, Comput. Methods Appl. Mech. Engrg., 33, (1982), 689–723.

[19] T.E. Tezduyar, M. Behr and J. Liou, *A new strategy for finite element computations involving moving boundaries and interfaces – The DSD/ST procedure: I. The concept and the preliminary numerical tests*, Comput. Methods Appl. Mech. Engrg., 94, (1992), 339–351.

[20] T.E. Tezduyar, M. Behr, S. Mittal and J. Liou, *A new strategy for finite element computations involving moving boundaries and interfaces – The DSD/ST procedure: II. Computation of free-surface flows, two-liquid flows, and flows with drifting cylinders*, Comput. Methods Appl. Mech. Engrg., 94, (1992), 353–371.

[21] A. Masud, T.J.R. Hughes, *A space-time Galerkin/Least-Squares finite element formulation of the Navier-Stokes equations for moving domain problems*, Comput. Methods Appl. Mech. Engrg., 146, (1997), 91–126.

[22] M. Lesoinne, C. Farhat, *Geometric conservation laws for flow problems with moving boundaries and deformable meshes, and their impact on aeroelastic computations*, Comput. Methods Appl. Mech. Engrg., 134, (1996), 71–90.

[23] F. Shakib, T.J.R. Hughes, *A new finite element formulation for computational fluid dynamics: IX. Fourier analysis of space-time Galerkin/least-squares algorithms*, Comput. Methods Appl. Mech. Engrg., 87, (1991), 35–58.

[24] T.J.R. Hughes, *The Finite Element Method - Linear Static and Dynamic Finite Element Analysis*, Dover Publishers, New York (2000).

[25] T.J.R. Hughes, G. Engel, L. Mazzei, and M.G. Larson, *The continuous Galerkin method is locally conservative*, J. Comput. Physics, 163, (2000), 467–488.

[26] C. Hirsch, *Numerical Computation of Internal and External Flows, Volume 1: Fundamentals of Numerical Discretization*, John Wiley & Sons, New York (1989).

[27] F.J. Blom, *A monolithical fluid-structure interaction algorithm applied to the piston problem*, Comput. Methods Appl. Mech. Engrg., 167, (1998), 369–391.

[28] C. Michler, S.J. Hulshoff, E.H. van Brummelen and R. de Borst, *A monolithic approach to fluid-structure interaction*, Computers and Fluids, (2003). (Accepted for publication). Preprint available at : `http://www.em.lr.tudelft.nl/~brummelen/publications.html`

[29] E. Kuhl, S. Hulshoff and R. de Borst, *An arbitrary Lagrangian Eulerian finite-element approach for fluid-structure interaction phenomena*, Int. J. Num. Methods Engrg., 57, (2003), 117–142.

[30] C. Michler, E.H. van Brummelen, S.J. Hulshoff and R. de Borst, *Efficiency of monolithic and partitioned methods for fluid-structure interaction*, in: Proceedings of the International Forum on Aeroelasticity and Structural Dynamics (IFASD), Amsterdam, The Netherlands, June 4-6 2003. Available at : `http://www.em.lr.tudelft.nl/~brummelen/publications.html`

List of Tables

Table 1
Parameters of the piston problem.

ρ_0	p_0	l_0	ω_{fs}	m	k
1.3	10^5	1.0	342	0.8	7911
$\frac{kg}{m^3}$	$\frac{N}{m^2}$	m	$\frac{1}{s}$	kg	$\frac{N}{m}$

Table 2
Observed order of temporal accuracy for partitioned and monolithic methods.

mesh sequences with time-step sizes	partitioned without prediction	partitioned with prediction	monolithic
$2^{-3},\ 2^{-4},\ 2^{-5}$	1.4667	1.9848	5.0188
$2^{-4},\ 2^{-5},\ 2^{-6}$	1.4565	1.9891	2.6159
$2^{-5},\ 2^{-6},\ 2^{-7}$	1.1958	2.0018	2.0457

Table 3
Observed order of temporal accuracy for trapezoidal and time-discontinuous Galerkin structural time integration in a monolithic solution.

mesh sequences with time-step sizes	trapezoidal method	time-discontinuous Galerkin method
$2^{-3},\ 2^{-4},\ 2^{-5}$	1.9541	3.0150
$2^{-4},\ 2^{-5},\ 2^{-6}$	2.0088	2.9925
$2^{-5},\ 2^{-6},\ 2^{-7}$	2.0019	3.0035

List of Figures

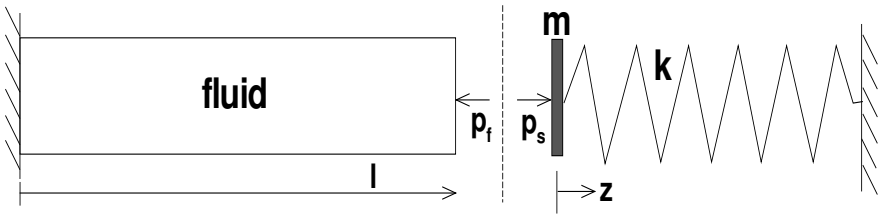

Figure 1. The piston problem (Interface region expanded for clarity).

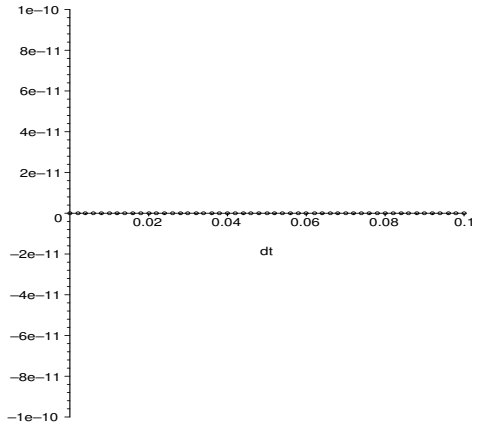

Figure 2. Amplitude error for trapezoidal time integration.

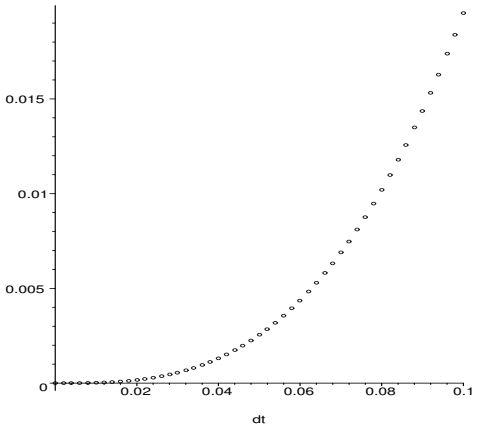

Figure 3. Phase error for trapezoidal time integration.

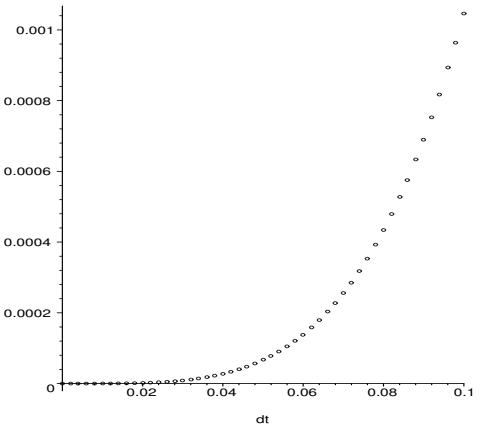

Figure 4. Amplitude error for discontinuous Galerkin time integration.

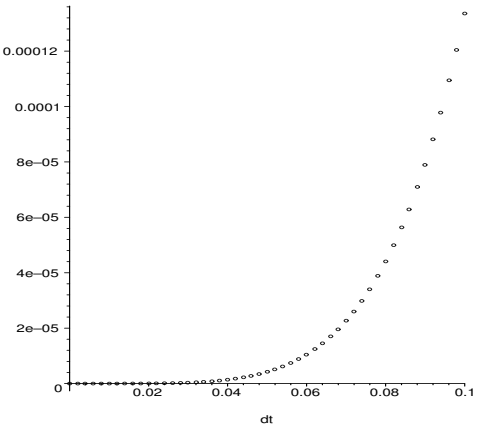

Figure 5. Phase error for discontinuous Galerkin time integration.

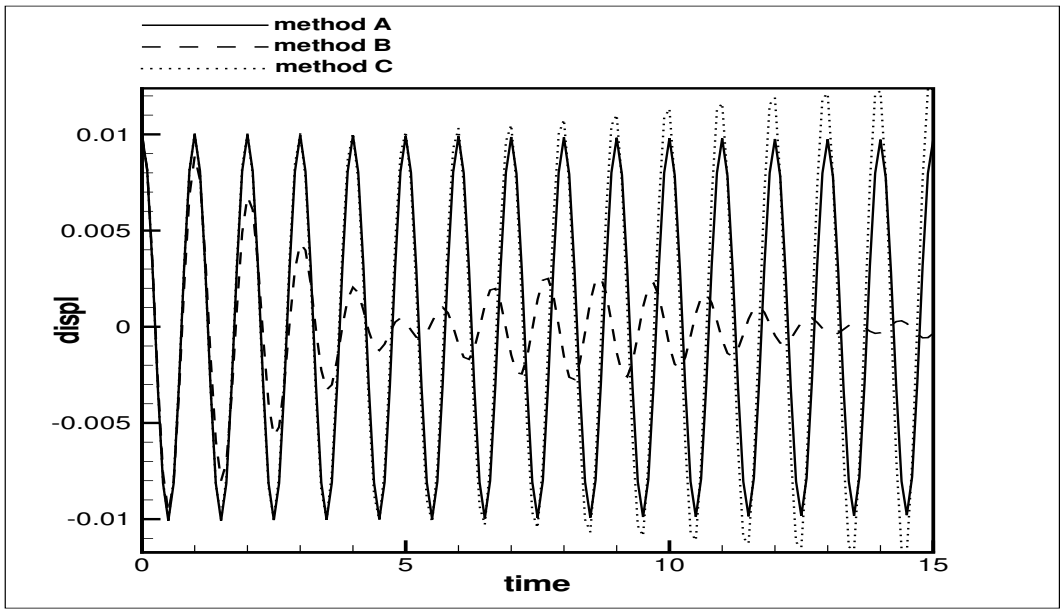

Figure 6. Structural displacement computed with the different coupling methods.

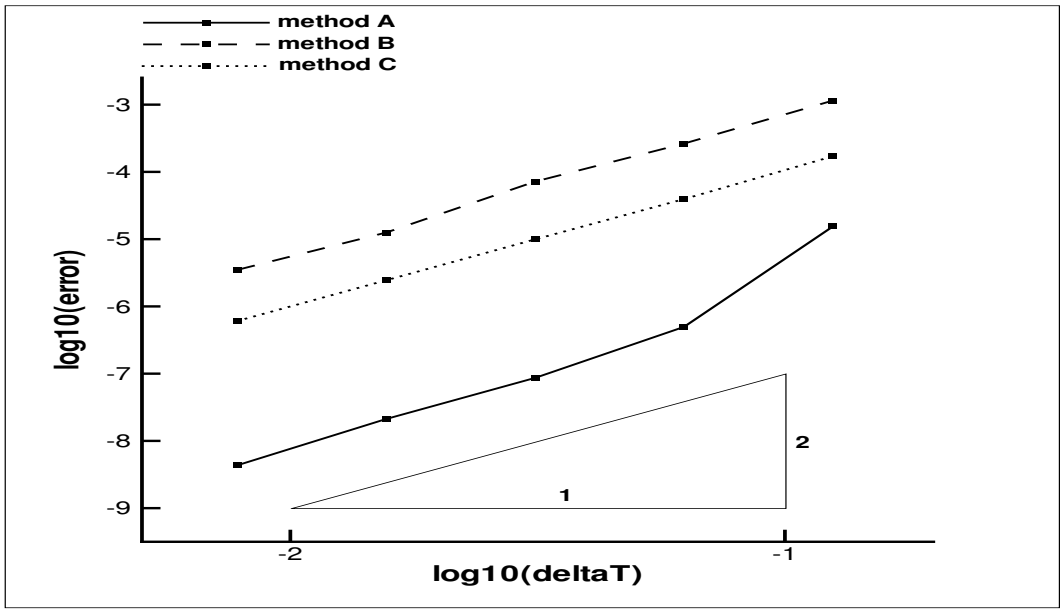

Figure 7. Error of the different coupling methods.

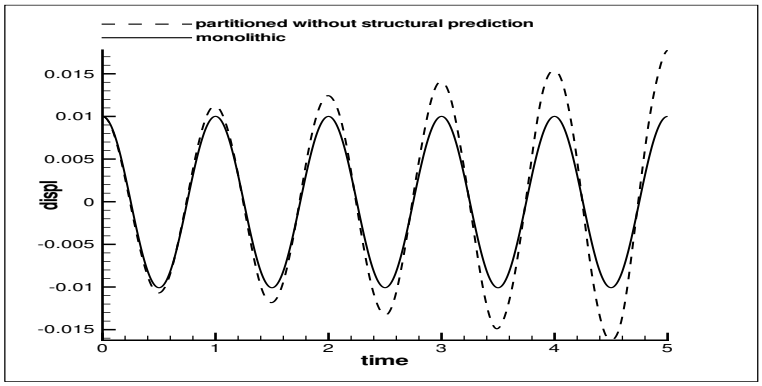

Figure 8. Structural displacement computed with a monolithic and a partitioned scheme without structural prediction, 100 time steps / cycle.

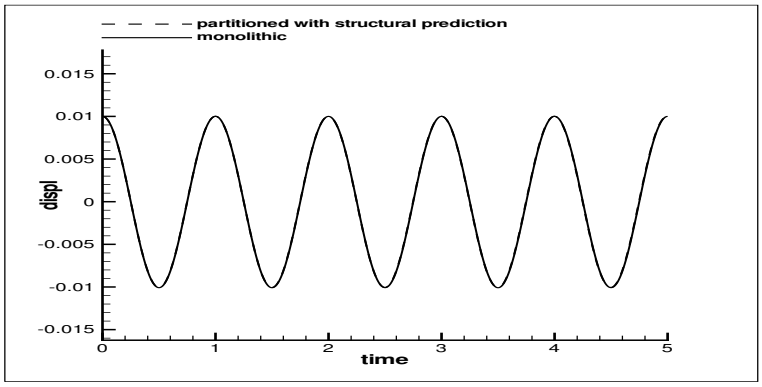

Figure 9. Structural displacement computed with a monolithic and a partitioned scheme with structural prediction, 100 time steps / cycle.

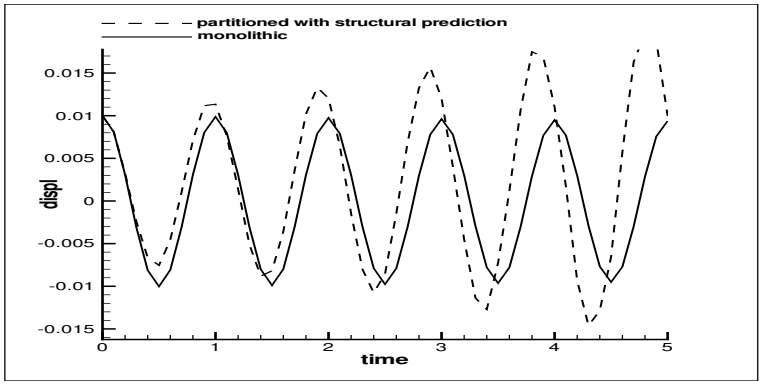

Figure 10. Structural displacement computed with a monolithic and a partitioned scheme with structural prediction, 10 time steps / cycle.

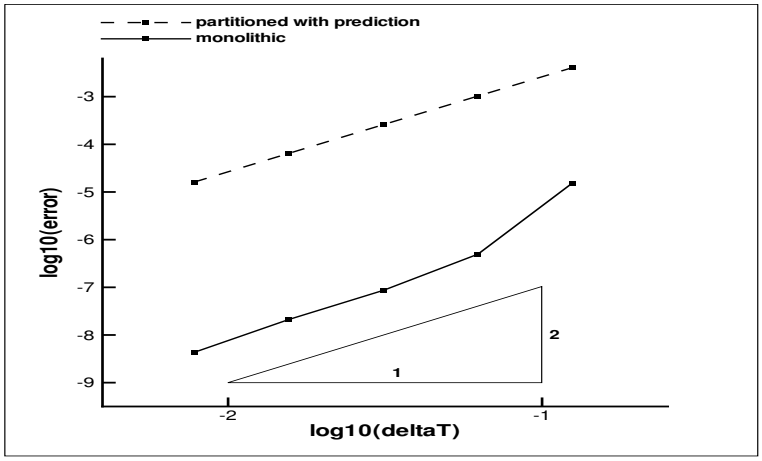

Figure 11. Error for a monolithic and a partitioned method with structural prediction.

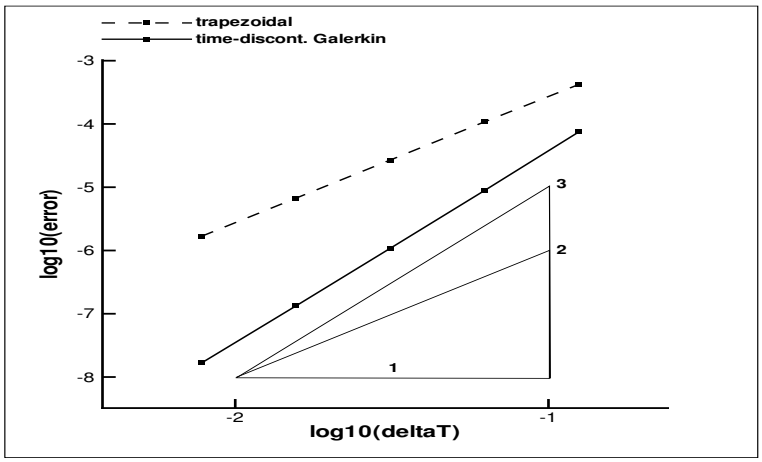

Figure 12. Error for trapezoidal and time-discontinuous Galerkin structural time integration in a monolithic solution.